Inteference of two high dimensional entangled photons

H.C.B. Florijn

August 31, 2009

Quantum Optics and Quantum Information group
This project was supervised by:
Dr. M.P. van Exter
Drs. H. Di Lorenzo Pires

Contents

1 Introduction

One of the most amazing features in quantum mechanics is entanglement. There is no such thing in our daily classical world that can be compared with this strange state in which particles can be. In quantum mechanics we can distinguish two broad categories of states; the separable states and the non-separable states. A separable state is a state where, for example, a two particle wave function can be written as a product of two one particle wave functions. With a non-separable state this cannot be done. Schrodinger called these kind of states entangled states [1], [2].

The best studied entangled state are the ones in 2 dimensions, like the spins or polarizations [3]. If you have for example 2 photons in a well defined polarization state in the horizontal or vertical bases the total wave function can be written as a product of both individual wave functions [2]:

$$\begin{aligned} |\Psi\rangle = |\Psi\rangle_a|\Psi\rangle_b &= (\alpha_a|H\rangle + \beta_a|V\rangle) \times (\alpha_b|H\rangle + \beta_b|V\rangle) \quad (1) \\ &= \alpha_a\alpha_b|H\rangle|H\rangle + \alpha_a\beta_b|H\rangle|V\rangle + \quad (2) \\ &\quad \beta_a\alpha_b|V\rangle|H\rangle + \beta_a\beta_b|V\rangle|V\rangle \end{aligned}$$

But for two entangled photons there is a strong correlation in polarization. If one photon has polarization 'H' the other should have 'V', a measurement of the polarization of one, also fixes the others. The total wave function cannot be written as a simple product of both individual wave functions [4], [5]:

$$|\Psi\rangle = \alpha_1|H\rangle|V\rangle + \alpha_2|V\rangle|H\rangle \quad (3)$$

Entangled photons play an important role in many quantum information processing technologies but most of the time only the 2 dimensional characteristics, like polarization, is taken into account. With the help of the Orbital Angular Momentum (OAM) of photons, entanglement in high dimensions can be used [3].

Entanglement in higher dimensions than two has many advantages in quantum information and quantum cryptography. It provides high dimensional alphabets for quantum information [6] and offers a better security against eavesdropping from unauthorized listeners [7].

Photon pairs entangled in OAM can be produced via the process of Spontaneous Parametric Down-Conversion (SPDC). In this process a single high-

frequency photon from an intense pump laser interacts with a nonlinear crystal. Here it generates two low-frequency photons, which can be entangled in polarization as well as in OAM. This is a reliable, but inefficient source for entangled photons [8].

In this report we investigate the distribution of OAM entangled states. We experimentally obtain the OAM or l-spectrum of entangled two photon states generated by SPDC. With this information we can calculate the amount of (azimuthal) spatial entanglement. The importance of our experiment is illustrated in the literature.

> "An experiment aimed at detecting the global OAM of the down-converted photon is a significant experimental challenge that is yet to be solved" [9]

In this Bachelor thesis I will show you how we have dealt with this challenge and offer some great results.

2 Theory: High Dimensional Entanglement in a Mach-Zener interferometer

In our experiment we are using type II Spontaneous Parametric Down Conversion (SPDC) in order to obtain two entangled photons. For an overview of our setup see Fig.1. The fields generated during the SPDC process are entangled in their orbital angular momentum [3]. This implies that their wave function can be written as [10]:

$$|\Psi\rangle = \sum_{l=-\infty}^{l=\infty} \sqrt{P_l}|\ -l\rangle|l\rangle \quad , \tag{4}$$

where P_l is the probability to generate a photon pair with Orbital Angular Moment $\pm l$, $|l\rangle$ denotes the OAM eigenmode of one photon,$\sum_{l=-\infty}^{l=\infty} P_l = 1$ and we have included the phases in the definition of $|l\rangle$ [11].

In type II SPDC both photons have orthogonal polarization, so we can split the two photons with a polarizing beam splitter (PBS). If the photon with OAM $-l$ is transmitted to arm 1, the photon with OAM l is reflected to arm 2, see Fig.1 where arm 2 is the arm with the rotator. When a photon in state $|l\rangle$ is reflected by a dielectric mirror the state after reflection becomes $i|-l\rangle$, i.e., a phase factor is added [4] and the orbital angular momentum is changed from l to $-l$ [12]. A $\frac{\lambda}{2}$-plate is added in one arm to make the polarization of both photons equal so the can interfere at the second beam splitter of Fig.1.

Next we determine the two-photon state in front of the second beam splitter with the image rotator oriented at angle $\theta = 0$. We call the photon in arm 1 with angular momentum $-l$: $|-l\rangle_1$ It hits 4 reflective surfaces, including the first beam splitter, so its state will be $i^4|(-1)(-1)^4 l\rangle_1 = |-l\rangle_1$. If both arms had the same amount of reflection surfaces, including the beam splitter and the 3 mirrors inside the image rotator and reflector (see Fig.1 and Fig.2), all phase factors cancel each other so the total state of the two photons just before they enter the second beam splitter is given by:

$$|\Psi\rangle = \sum_{l=-\infty}^{l=\infty} \sqrt{P_l}|\ -l\rangle_1|l\rangle_2 \quad , \tag{5}$$

where $|l\rangle_2$ stands for a photon with angular momentum l in arm 2. We call this arrangement, where photon pairs with different sign of OAM are

entering the beam splitter, the *odd* configuration.
But instead we placed an extra mirror in arm 2 and due to this mirror the state right in front of the the second beam splitter can be described as:

$$|\Psi\rangle = \sum_{l=-\infty}^{l=\infty} \sqrt{P_l} i|\ -l\rangle_1|-l\rangle_2 \tag{6}$$

This arrangement, where photon pairs with the same sign of OAM entering the second beam splitter, is called the *even* configuration.
By rotating the beam we add a factor $e^{-il\theta}$ [12] to the photon in arm 2 so the wave function is written as:

$$|\Psi\rangle = \sum_{l=-\infty}^{l=\infty} \sqrt{P_l} i e^{-i\theta l}|\ -l\rangle_1|-l\rangle_2 \tag{7}$$

When both photons hits the second beam splitter they can choose different directions. The photon in arm 1 can be transmitted to arm 3 or reflected to arm 4 and the photon in arm 2 can be reflected to arm 3 or transmitted to arm 4 so the total output wave function will be:

$$\begin{aligned} |\Psi_{out}\rangle &= (\frac{1}{\sqrt{4}}) \sum_{l=-\infty}^{l=\infty} \sqrt{P_l}(i e^{-i\theta l}|-l\rangle_3|-l\rangle_4 + i^3 e^{-i\theta l}|l\rangle_3|l\rangle_4 & (8)\\ &\quad + i^2 e^{-i\theta l}|-l\rangle_3|l\rangle_3 + i^2 e^{-i\theta l}|l\rangle_4|-l\rangle_4) & (9) \end{aligned}$$

In our setup we are only interested in the case were both photons go to different ports of the beam splitter i.e., coincidence detection. So taking only the part of Eq.(8) where both photons go different directions and making use of $P_{-l} = P_l$ we can write the detection wave function as follows:

$$\begin{aligned} |\Psi_{det}\rangle &= (\frac{1}{\sqrt{4}}) \sum_{l=-\infty}^{l=\infty} \sqrt{P_l} i e^{-i\theta l}|-l\rangle_3|-l\rangle_4 + i^3 e^{-i\theta l}|l\rangle_3|l\rangle_4 & (10)\\ &= (\frac{1}{\sqrt{4}}) \sum_{l=-\infty}^{l=\infty} \sqrt{P_l} i(e^{-i\theta l} - e^{i\theta l})|l\rangle_3|l\rangle_4 & (11)\\ &= \sum_{l=-\infty}^{l=\infty} \sqrt{P_l} \sin l\theta |l\rangle_3|l\rangle_4 & (12) \end{aligned}$$

The number of coincidences is proportional to:

$$\langle \Psi_{det}|\Psi_{det}\rangle = \sum_{l'=-\infty}^{l'=\infty} \sqrt{P_l'}\sin(\theta l')_4\langle l'|_3\langle l'| \sum_{l=-\infty}^{l=\infty} \sqrt{P_l}\sin(\theta l)|l\rangle_3|l\rangle_4 \quad (13)$$

$$= \sum_{l'=-\infty}^{l'=\infty} \sqrt{P_l'}\sin(\theta l') \sum_{l=-\infty}^{l=\infty} \sqrt{P_l}\sin(\theta l)_3\langle l'|l\rangle_3\ {}_4\langle l'|l\rangle_4 \quad (14)$$

Since $\langle l'|l\rangle = \delta_{l',l}$ and $\sum_{l'=-\infty}^{l'=\infty} P_l = 1$ the number of coincidences, Eq. (14), becomes:

$$\langle \Psi_{det}|\Psi_{det}\rangle = \sum_{l=-\infty}^{l=\infty} P_l \sin^2(\theta l) \quad (15)$$

$$= \frac{1}{2}\sum_{l=-\infty}^{l=\infty} P_l(1-\cos(2\theta l)) \quad (16)$$

$$= \frac{1}{2} - \frac{1}{2}\sum_{l=-\infty}^{l=\infty} P_l\cos(2\theta l) \quad (17)$$

From Eq.(17) we can deduce the visibility V as a function of θ. The Visibility is given as [13]:

$$V(\theta) = \frac{(Max_{counts} - Min_{counts})}{Max_{counts}} \quad (18)$$

$$= \frac{1-(1-\sum_{l=-\infty}^{l=\infty} P_l\cos(2\theta l))}{1} \quad (19)$$

$$= \sum_{l=-\infty}^{l=\infty} P_l\cos(2\theta l) \quad (20)$$

In our experiment we measure the function $V(\theta)$ and from this we can find P_l using the Fourier transformation of $V(\theta)$.

$$V(\theta) = \sum_{l=-\infty}^{l=\infty} P_l \cos(2\theta l) \tag{21}$$

$$= \sum_{l=-\infty}^{l=\infty} P_l e^{i2l\theta} \tag{22}$$

With $P_{-l} = P_l$. We recognize Eq.(22) as a Fourier serie $V(\theta)$ so the only thing we have to do is transform this formula to obtain the coefficients P_l [14]:

$$P_l = \frac{1}{\pi} \int_{-\frac{\pi}{2}}^{\frac{\pi}{2}} V(\theta) e^{-i2l\theta} d\theta \tag{23}$$

Note that in the experiment we use a Fast Fourier Transform because the measured visibility is not continuous with θ but is discrete.The complex nature of this transform automatically makes $P_{-l} = P_l$ for the real valeud experimental data. From this we can calculate the effective number of modes [13] which is given by the Smidt number [12]:

$$K_{AZ} = \frac{1}{\sum_l P_l} \tag{24}$$

So we can see that performing our experiment and some little algebra we can find the number of dimensions from the OAM Hilbert space.

3 The Experiment

3.1 Setup

Now we are left with the experimental challenge to measure the coincidences and find the probability distribution for the orbital angular momentum of the entangled photons. An overview of the setup can be seen in Fig.1.

We use a $413,1$ nm Krypton-Ion laser as a pump laser. A $f = 1000$ mm lens is used to focus the pump laser in the crystal to a width of 150 μm. The laser beam is reflected by a piezo mirror. At the backside of this mirror there are two piezo elements which allows us to control the angle of this mirror

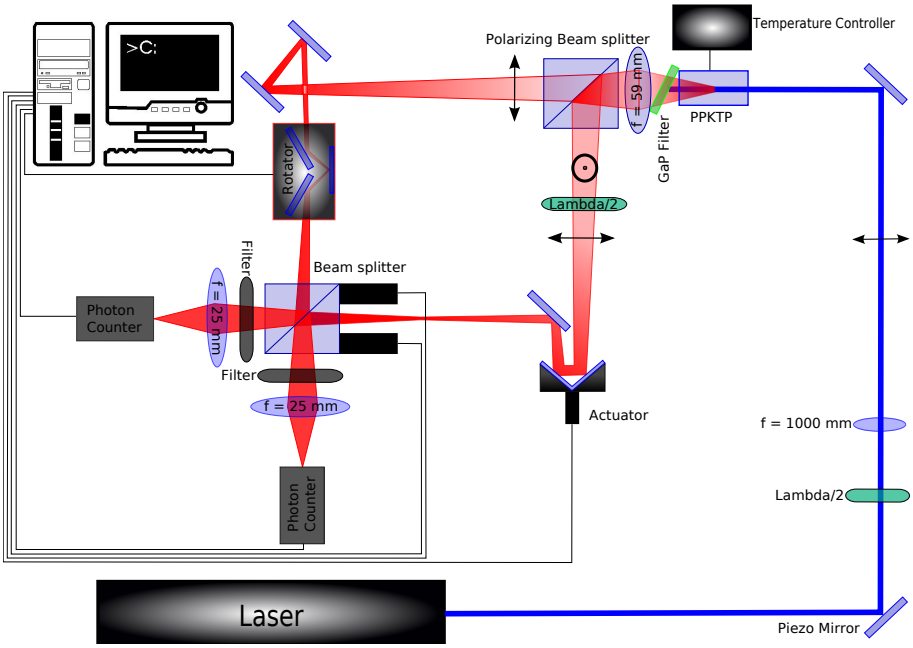

Figure 1: *Schematic drawing of the setup.*

with help of a feedback system. A small part of the beam is reflected by a wedge to a quadrant detector, which is located at the same distance from the pump as the crystal is. If the beam is not on the right position, the detector gives a signal that we use to align piezo mirror. A $\lambda/2$ plate is used to rotate the polarization of the pump to horizontal.

The temperature of the crystal is controlled by a Peltier element. The crystal is a 2 mm periodically-poled KTP crystal, poled for type II spontaneous parametric down conversing. This crystal converts, with very low efficiency, one photon of the pump laser into two photons with half the frequency of the the pump laser. So $\omega_{pump} = \omega_s + \omega_i$ where 's' and 'i' stands for 'signal' and 'idler'. The photons are entangled in orbital angular momentum, if one has orbital angular momentum 'l', then the other has '$-l$'. The polarization of the two entangled photons is opposite, so we can easily separate them with a polarizing beam splitter. We use a GaP-filter right behind the crystal to block the pump light.

A $f = 59\ mm$ lens is used to make an image, of the pumped region of the PPKTP, right in front of the rotator with a magnification of 13×. More

details concerning the size of the spot in the rotator and the movement of spot is given in the next section.

The vertically polarized part of the beam is reflected in the first beam splitter. There we placed a $\lambda/2$ wave plate to rotate the polarization to horizontal so it can interfere with the light coming from the other arm of the interferometer.A computer controlled actuator in combination with 3 mirrors is used to make both arms of the interferometer the same length.

In the other arm of the interferometer, arm 2, there is a combination of 2 mirrors and an image rotator and reflector (IRR). The IRR is used to rotate the image and because it contains 3 mirrors it reflects the image as well. Furthermore we see that we have 1 reflective surface more in arm 2 then in arm 1.

In the middle of the second beam splitter both photons meet and then they "decide" which side they go following the rules described in the theoretical part. To make sure that both beams of the interferometer are right on top of each other we have installed micrometer screws on the first beams splitter. To ensure that both beams are leaving the second beam splitter parallel we placed 2 computer controlled actuators on this beam splitter. After the second beam splitter both beams encounter a 2 nm bandpass filter centered at 826.2 nm to select only frequency-degenerate photons.

Then we see two $f = 25$ mm lenses focus the beam on the sensitive surface of the photon counting modules. These surfaces have a diameter of 180μm. Both modules produces a TTL pulse with a width of $\simeq 30$ ns and are connected with the computer so we can record the single counts and the coincidences using a fast AND gate with a 1.7 ns gate time window.We have computerized a lot of our setup to get the precision in alignment needed for succeeding in our task to find the coincidences as a function of angle of the IRR. More details on the alignment needed is given in the next section.

3.2 The Image Rotator and Reflector (IRR)

The hardest part of our experiment, or the part that took most of our time, was aligning the IRR. The image rotator and reflector, from now on simply called *rotator*, is a key part of our setup, the success of our experiment strongly depends on a good alignment of this device. Based on the expected 'fine-structure' within the beam we estimate that the movement of the spot must be less than 10% of the size spot in order to maintain the quality of interference. The width of the spot in the crystal is 150μm. We us a

$f = 59$ mm lens to make a 13× magnified image right in front of the rotator. Consequently the width of the beam at that position will be 1950μ m. So the movement of the beam in the rotator, the near field, must be less than 195μm. In the far field we have calculated that the maximum movement of the output angle of the beam must be less then 160 μrad. This number is based on the divergence angle of the pump laser, the opening angle of the SPPC radiation and the magnification of 13×.

The image rotator and reflector (IRR) consists of a box with 3 mirrors inside that is rotating around its horizontal central axis.[see Fig.2]

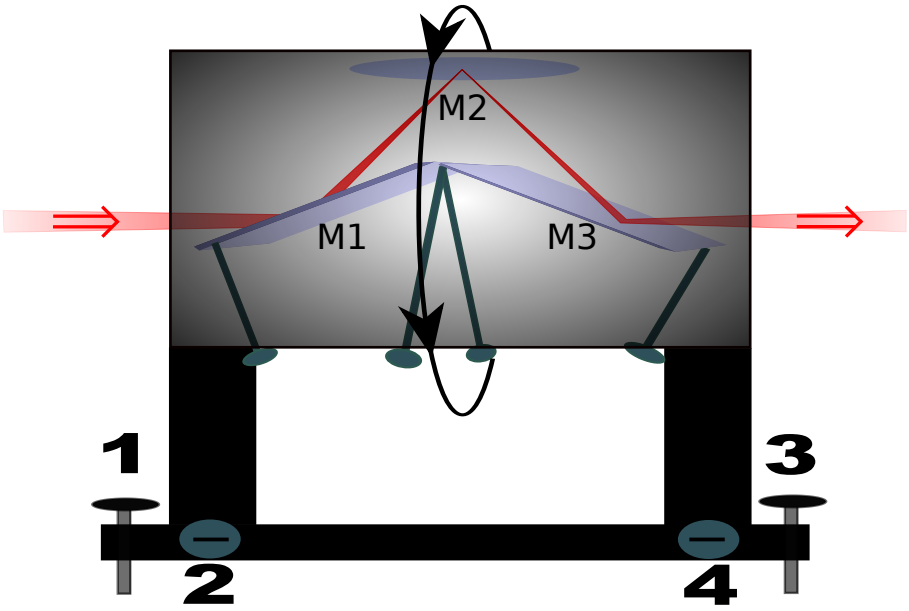

Figure 2: *Artistic impression of the image rotator and reflector. Three mirrors are seen, two movable mirrors in the front and back and an fixed mirror in the middle. The whole black box is rotating with help of a motor, controlled with the computer. Its position on the table can be adjusted with help of the four screws.*

The rotator itself has 4 screws as well. If you move screws 1 and 3 by the same amount you can adjust the vertical position y of the rotator, if you move screws 2 and 4 you can adjust the horizontal position x of the rotator. By moving only screw 1 or 3 you can adjust the vertical angle of the rotator (θ_y) and by moving only screw 2 or 4 you can adjust the horizontal angle

(θ_x). In total we can adjust 8 screws in order to align the rotator.

But how can we navigate in this 8 dimensional space? Well we can make it a little bit easier by switching between the near field (nf) and the far field (ff). We do this by building a $2f-2f$ imaging system (nf) or a $f-f$ imaging system (ff). This was done by placing a flip mirror after the second beam splitter, block the beam in arm 1, remove the filter behind the crystal, place a camera, the Spiricom or the ICCD, at a distance of 120 cm behind the rotator and use a lens of $f = 60\ cm$ for the ff or a $f = 30\ cm$ for the nf.[see Fig.3]

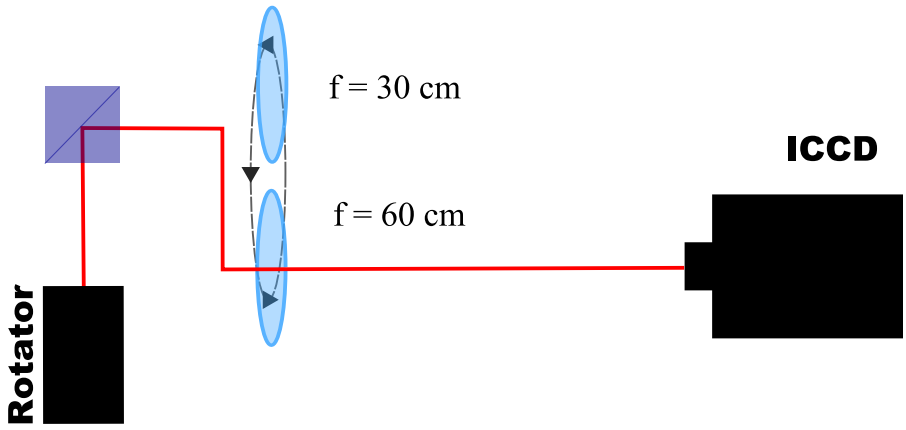

Figure 3: *The imaging system.To see the farfield, place the $f = 60$ cm lens. Place the $f = 30$ cm lens for the nearfield. Instead of an ICCD camera we have also used a Spiricom with the light of the pump laser in combination with some filters.*

If we look at the nf we can ignore the misalignment in the angles of the rotator and the misalignment of the third mirror in the rotator. We image the position of the beam on mirror 3, so we look at the angle of mirror 1 and the position of the rotator on the table. If we are in the ff the image is more sensitive to changes in angles then in position, so we can concentrate on moving the screws from the third mirror and only one set of screws on

the rotator.

3.3 Aligning the Image Rotator and Reflector

But how do we know if we have to change the screws on the rotator or those of the mirrors? For that we made a simulation based on Fig.4 to see how the movement of the output beam during rotation depends on various angles and positions. As you can see we are looking at the far field, let's suppose that only the third mirror and angle of the rotator are misaligned in one direction, see Fig.4.

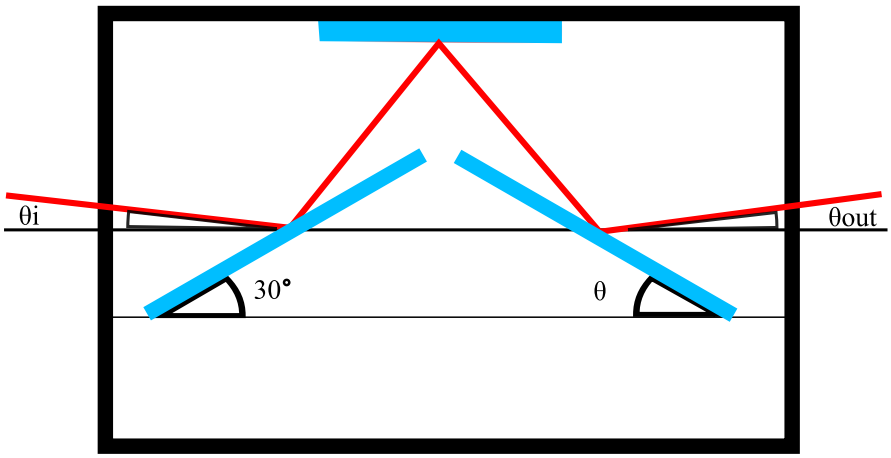

Figure 4: *Picture to help us find a relationship between the output angle of the rotator and the angle of the rotator and the third mirror.*

From this picture we can deduce the following relation between input angle (θ_i), output angle (θ_{out}) and the angle of the third mirror (θ):

$$\theta_{out} = 2\Delta\theta + \theta_i \tag{25}$$

With $\Delta\theta = \theta - 30^o$ is the misalignment of the third mirror with respect to the axis of the rotator and θ_i is the misalignment of the rotation axis of

the rotator with respect to the incoming beam, the lab frame, and θ_{out} is also in the lab frame of reference. Now we want to see what happens with the beam if you rotate the rotator around its axis of rotation. To do so we use polar coordinates (r, ϕ) to write the movement as function of angles:

$$\begin{aligned} \hat{r} &= r\sin(\theta_i)\hat{x} + r\sin(\theta_{out})\cos(\phi)\hat{x} + r\sin(\theta_{out})\sin(\phi)\hat{y} && (26) \\ &= r\sin(\theta_i)\hat{x} + r\sin(2\Delta\theta + \theta_i)\cos(\phi)\hat{x} + r\sin(2\Delta\theta + \theta_i)\sin(\phi)\hat{y} && (27) \end{aligned}$$

Next, we make use of the facts that when $2\Delta\theta = 0$ then $\theta_{out} = \theta_i$ and $\phi \Longrightarrow 2\phi$. Therefore:

$$\hat{r}(\Delta\theta = 0) = r\sin(\theta_i)\hat{x} + r\sin(\theta_i)\cos(2\phi)\hat{x} + r\sin(\theta_i)\sin(2\phi)\hat{y} \quad (28)$$

And we use that when $\theta_i = 0$ then $\theta_{out} = 2\Delta\theta$, so:

$$\hat{r}(\theta_i = 0) = r\sin(2\Delta\theta)\cos(\phi)\hat{x} + r\sin(2\Delta\theta)\sin(\phi)\hat{y} \quad (29)$$

Which leads to a $\hat{r}_{total}$ of:

$$\begin{aligned} \hat{r}_{total} &= r\sin(\theta_i)\hat{x} + \hat{r}(\Delta\theta = 0) + \hat{r}(\theta_i = 0) && (30) \\ &= r(\sin(\theta_i)\cos(2\phi) + \sin(2\Delta\theta)\cos(\phi))\hat{x} && (31) \\ &\quad + r(\sin(\theta_i)\sin(2\phi) + \sin(2\Delta\theta)\sin(\phi))\hat{y} \end{aligned}$$

For small angles we can make the following approximation for Eq.(31):

$$\hat{r}_{total} \sim (\theta_i + \theta_i\cos(2\phi) + 2\Delta\theta\cos(\phi))\hat{x} + (\theta_i\sin(2\phi) + 2\Delta\theta\sin(\phi))\hat{y} \quad (32)$$

If we plot the relationship from Eq.(32) in Matlab, we get the pictures of Fig.5.

We see that if we have 2 circles we know that the mirror is misaligned, the more this mirror is misaligned, the bigger the difference between both circles. The size of the biggest circle tells us how bad the rotator is misaligned (for an experimental picture see Fig.6). Note that a 180^o turn of the rotator corresponds with a 360^o rotation of the beam. From the simulation done above we can develop a procedure to align the rotator which, will be given in the next section.

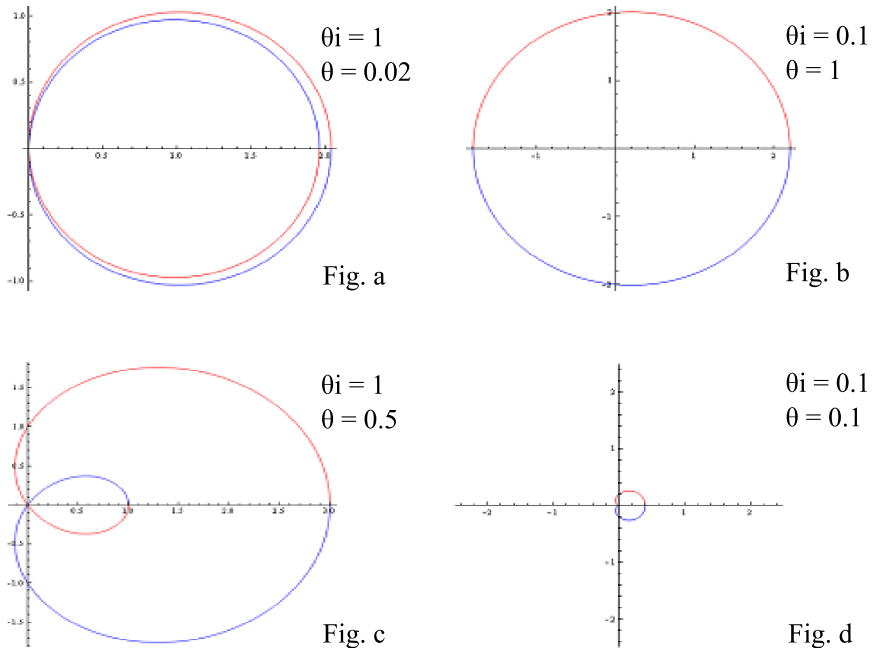

Figure 5: *In a) we see a big misalignment in the rotator because of the size of both circles and a small misalignment in the mirror because both circles almost coincide. In b) we see a big misalignment in the mirror, this is so big that it looks like one circle. When you do the experiment and track the laser beam with a camera you will notice that it stays on one position for some time, the spot makes a circular motion around its center point here and after this it will follow the big circular motion. In Fig. c we see a big misalignment in the rotator, what results in a big circle and a misalignment in the mirror, what results in a smaller circle. In Fig. d both rotator and mirror are reasonably good aligned and we see more or less one small circle.*

We have used a Spiricom camera or an ICCD camera to align. When we implement the Spiricom we could use the pump laser to align. For this we placed the Spiricom on the position of the ICCD, Fig.3, and took away the GaP-filter that blocks the pump laser. Furthermore we implemented some neutral density filters so we don't destroy the Spiricom. We used the Spiricom because the software of this camera has an option to follow the center of mass of the spot. This gave us more accuracy in the position of the beam and we could make nice pictures of the spot while rotating the rotator in order to see the movement of the beam, Fig. 6, and see the circles

described above.

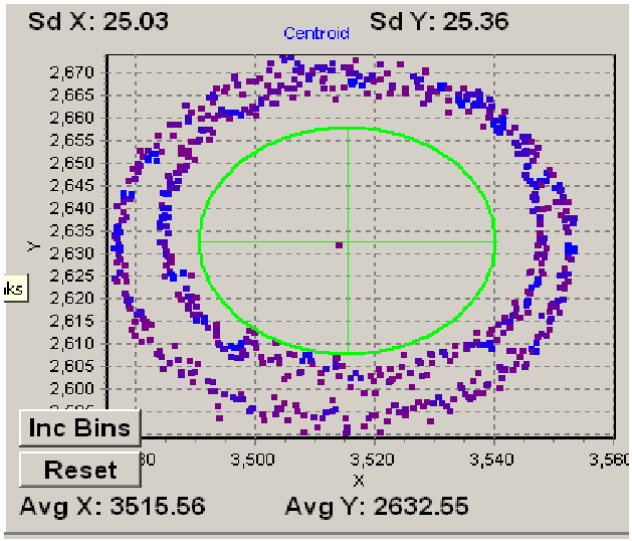

Figure 6: *In this picture we rotated the image rotator and reflector* 360^o*. We looked at the near field and tracked the center of mass of the spot. Clearly seen are two circles, so we know that the first mirror is misaligned and from the size of both circles we know that the position of the rotator can be adjusted as well. Note that the scale of the Spiricom pictures are in* μm*.*

Using the formula,

$$\theta_{out} = \frac{\Delta x}{f} \tag{33}$$

and the picture made by the spiricom we can easily calculate θ_{out}, which is a measure for the alignment of the rotator. From Eq.(33) we calculate that $\theta_{out} = \frac{80\ \mu m}{30\ cm} = 270\ \mu rad$.

So now we have all the tools to align the rotator. However we found out that during the day the laser was drifting so we could not align the rotator and make a scan because during the scan the beam moved. So we had to find a solution for this. We implemented a feedback loop in order to fix the position of the laser on the crystal, see section 4.5. In our best efforts, with the feedback loop, we found a misalignment in the near field of less then 20 μm and for the far field of 80 μm (at $f = 60$ cm) which via Eq.(33) corresponds to an anlge of 140 μrad [Fig.7]. So both in the near field and in the far field we have the alignment we need for our measurement. Further

optimization is not possible due to mechanical deficiencies of the rotating device as can bee seen in Fig.8. Note that the best image rotators available on the market are dove prism with a an angle tolerance of 900 *mrad*.

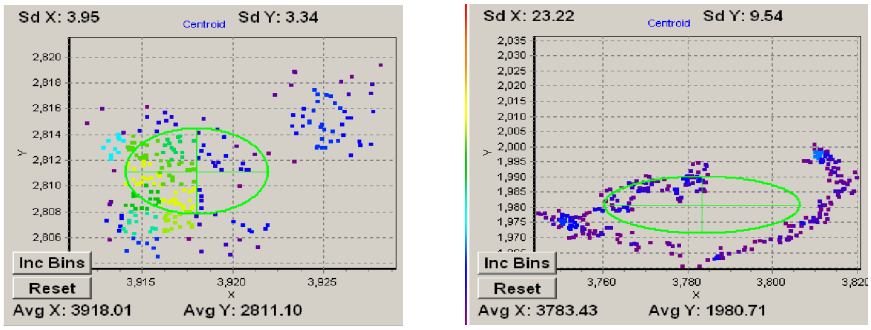

Figure 7: *Left:The near field, we found a misalignment in the x and y position of* 20 μm *when we rotated the rotator by* 90^o *. Right: The far field, where we have found a* $\Delta x = 80$ μm *and a* $\Delta y = 40$ μm *in a* 90^o *rotation of the rotator.*

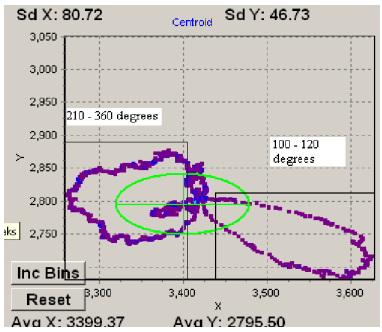

Figure 8: *A picture of a full rotation in the far field. Clearly seen are the two strange lobs which we think are due to mechanical deficiencies of the image rotator and reflector, in the final measurements we never made a full turn to avoid these lobs.*

3.4 Align the rotator in less then 10 steps

1) Look at the nf and see what kind of a figure you have.
2) Make both circles coincide with help of the two screws of mirror 1.
3) Make circle as small as possible by marking the spot, then rotate the image rotator 90^o and bring the spot back to x-position of the marked point using screw 2 and 4.
4) Mark this point, then rotate back to 0^0 and bring the spot back to the y-position of the marked point using screw 1 and 3.
5) Switch to the ff
6) Make both circles coincide with help of the two screws of mirror 3.
7) Make circle as small as possible by marking the spot, then rotate 90^o and bring the spot back to x-position of the marked point using screw 2 or 4.
8) Mark this point, then rotate back to 0^0 and bring the spot back to the y-position of the marked point using screw 1 or 3.
9) Repeat steps 1 till 8 until you have the alignment you need

3.5 Feedback loop

As mentioned the laser beam was drifting during a certain time and this resulted in big problems concerning our alignment. In order to have a more stable beam we use a feedback loop. Our feedback loop consists of a quadrant detector with control box, a wedge, two Proportional Controllers (one for the x position and the other for the y position), two Integral Controllers, oscilloscope, and one Piezo Mirror with a P-836 piezo driver. We used only one Piezo mirror and one quadrant detector because we wanted to keep the location of the pump spot on the PPKTP fixed; not it's precise angle.

The quadrant detector has an 2×2 array of individual photodiode active area's separated by a small gap, fabricated on a single chip. The quadrant detector calculates the difference between all four quadrants. So if the laser hits the center, the right side minus the left side will be zero and the upper side minus the lower side will be zero. If this is not the case an output voltage will be generated for the horizontal difference and for the vertical difference. The detector has 2 outputs so we can extract the x and y position of the beam. For convenience we connected these two outputs to the oscilloscope for monitoring. And from the oscilloscope we connected both wires to the PI controller. With these controllers we can give a set value, we choose this to

be 0 Volt, because that is the voltage the detector returns when the laser hits the center of the detector. If the laser doesn't hit the center of the detector, it gives a voltage. The difference between this voltage and the set value is called the error. The PI-controllers manipulate this error voltage and steers a signal to the piezo driver to change the angle of the mirror in order to make the laser hit the center of the detector. This process of measuring the position of the beam and steering the piezo mirror is continuously happening. The manipulation of the Proportional controller is the following:

$$V_{out} = \varepsilon(t) \times K_p \tag{34}$$

And for the Integrating Controller:

$$V_{out} = \frac{K_i}{\tau} \int_0^t \varepsilon(t')dt' \tag{35}$$

Where the constants K_p, K_i, and the integration time τ are values to be determined by trail and error. After finding the correct values we made a 60 minute scan of the beam and we can see in Fig. 9 that the spread of the center of mass in the x position is less then 25 μm and in the y position is less then 18 μm.

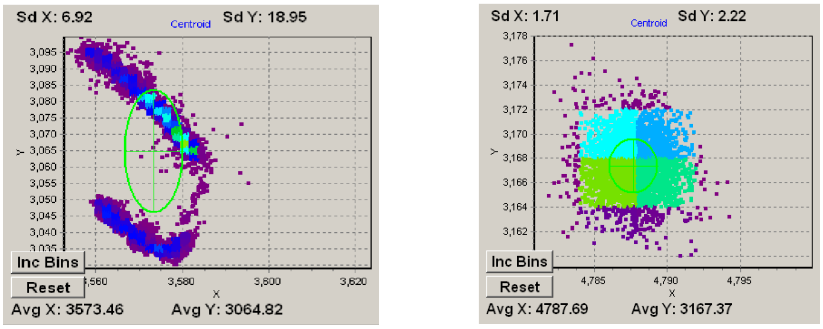

Figure 9: *Left: the movement of the spot at a distance comparable to the distance from the crystal to the center of the rotator during a time period of 25 minutes without feedback loop. We can clearly see that the spot has moved more than* 60 μm *in the y position. Right: With feedback loop the maximum variation in positions is only about* 25 μm *in the x position and* 18 μm *in the y position.*

3.6 Aligning the complete setup

Now we know how to align the rotator it is time to align both beam splitters. This is of crucial importance to have good interference. What we want is that both beams in the second beam splitter are exactly on top of each other and parallel. In order to do so we use the same trick as with the rotator, we make an image of the near field of the beam splitter and of the far field. The near field is the position of the beams in the second beam splitter. If both beams are on top of each other in the near field and far field then we know also that both beams are leaving the second beam splitter parallel.

To investigate the near field we place a $f = 25$ cm lens between the second beam splitter and the ICCD. The distance between the ICCD and the second beam splitter is 100 cm. For the far field we insert an $f = 50$ cm. Because we use only moveable and flip lenses we can easily switch between the far field and near field from the beam splitters and because we are using the same kind of lenses for the image system of the rotator we can easily switch between the fields of the rotator and the beam splitters.

To get a very accurate measure of position we wrote a labview program to calculate the center of mass of the SPDC-beam for the ICCD camera, so the final alignment is done using the SPDC-light! What we do now is look at the near field, block the arm that is reflected from the first beam splitter, arm 1, and note the position of center of mass (COM). Then block arm 2 and move the spot with help of the micrometer screws on the first beam splitter to the COM of arm 1. Now the beams are almost exactly on top of each other within a region of 30 μm because this is the spread in position of the beam.

Now we look at the far field and block the arm that is transmitted by the first beam splitter, arm 2. Make a note of the position of the beam from arm 1. Block arm 1 and move the spot of arm 2 to the noted position of arm 1 with help of the actuators on the second beam splitter. Repeat this procedure several times because by changing angle of the the second beam splitter you also change the position of the two beams in the second beam splitter a little bit.

Now we make sure the beams are focused exactly on the 180 μm wide sensitive areas of the photon counters. The size of the spot due to the $f = 59$ mm lens is 1950 μm and we focus this image on the detector with help of the $f = 25$ mm lens. The distance between this image and the $f = 25$ mm lens is around 50 cm so the image will be demagnified 19$\times$. The spot size on

the detector then will be $\frac{1950\ \mu m}{19} \approx 100\ \mu$ m so we are sure that we collect all the light if we place the $f = 25$ mm lens with its focus at the detector. We optimized the position of the lens with the help of this detector to find a maximum value for the single counts.

Our final task is to find the position of the actuator in arm 1 to make both arms of the same length. We do this with help of a diode laser with a wavelength of 826 nm which follows exactly the same path of the generated SPDC light. We place a photo detector at one of the output arms of the second beam splitter. To find the optimum position of the actuator we look at which position the voltage is the maximum, here we have constructive interference and both arms are of the same length.[see Fig. 10] To have a very accurate position we use the laser below threshold so the diode laser has a very low coherence. Now everything is aligned we can start our measurements.

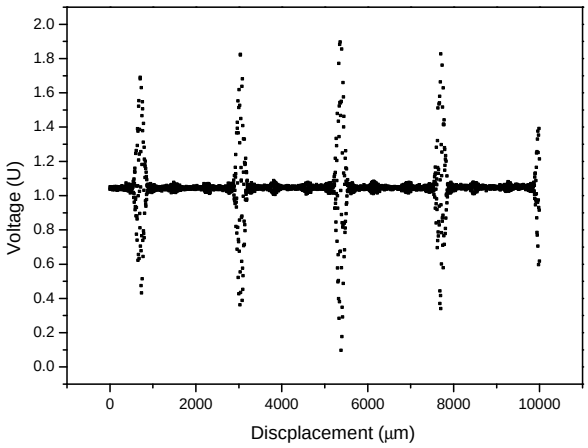

Figure 10: *A measurement to find the optimum position of the actuator. For good interference we should place the actuator at* 5350 μm*. The power of the laser was* 0.08 mW*, which is below threshold, in order to have a low coherence.*

4 Results

4.1 Even-configuration

In our measurements we looked at two different situations,we can take away the mirror right in front of the rotator to get photon pairs with a different sign for OAM at the second beam splitter, the even configuration. Or we can investigate the odd-configuration, with the mirror in front of the rotator. As explained in the theocratical part, using the odd-configuration we should see a visibility that depends on the angle of rotator, where as for the even-configuration we should see no dependency, only a constant visibility.

We started doing measurements without the extra mirror, ie, in the even-configuration. When we aligned everything we made a scan of the coincidences while moving the rotator to see a beautiful dip at the position where we have interference, Fig.11. We placed the rotator at a fixed position and only moved the actuator. All measurements were done at a crystal temperature of 15^oC, where we have optimum phase matching.

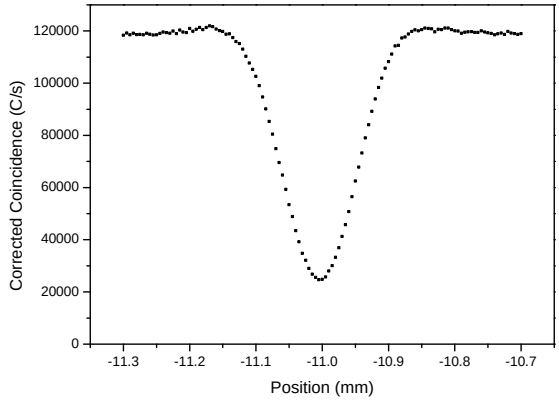

Figure 11: *A measurement of the coincidences while moving the rotator where the coincidences are corrected using Eq.*(36)*.The dip due to the interference of the entangled photons is clearly visible. When the actuator is at position around* -11.0 *mm both arms of the interferometer have the same length.*

We place then the actuator on the position of the dip and make a scan of the coincidences when rotating the image rotator. We did this automatic (with help of a motor) and manual, where we aligned for every point.[see Fig.12]

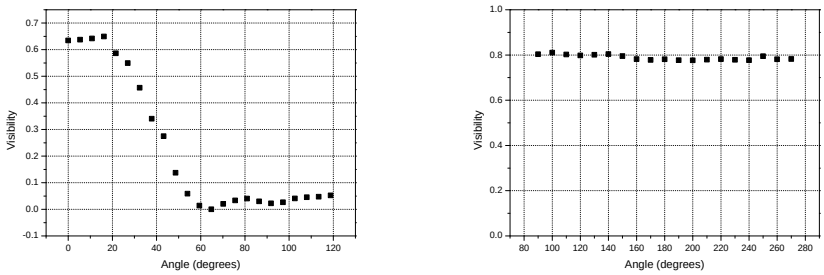

Figure 12: *Two-photon visibility versus rotation angle for automated scan (left) and manual scan (right). The visibility decreases rapidly in the automated scan. The visibility is almost constant in the manual scan, where we aligned for every point.*

We see that the coincidences as a function of angle hardly changes when we aligned for every point and is almost constant. In the automated scan the visibility decreases rapidly, within a 60^o rotation of the image the visibility drops to zero. This may be caused by the shaking of the motor on the table. When rotating the rotator becomes more and more misaligned.

4.2 Odd-configuration

If we change now to the setup were we have one extra reflective surface in arm 2 we should see a visibility $V(\theta) = \sum_{l=-\infty}^{l=\infty} P_l \cos(2\theta l)$, as described in the theoretical part. The visibility should have a drop, see Fig.13, at places where $2\theta l = n \times \pi$, with $n = 0, \pm 1, \pm 2, \pm 3, ..., ..., etc$ so the drop will repeat itself every 180^o, see Fig.14.

If two photons accidentally arrive within a time window of 1.7 ns at both detectors, the 'AND' gate of the electronics will also measure this as a coincidence, because within this time window there is a finite statistical chance of coincidence detection of photons that are not a truly pair. This is

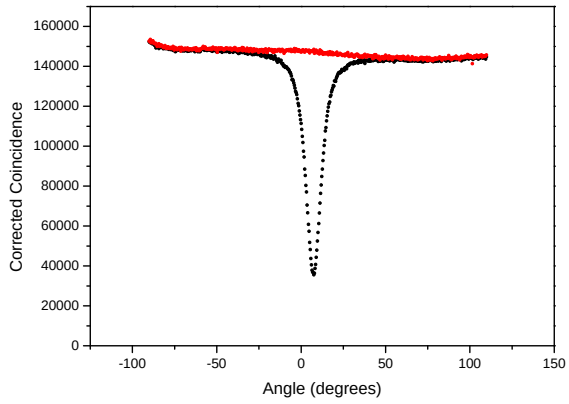

Figure 13: *A* 180^o *scan of the coincidences in the odd-configuration. In red we see the corrected coincidences* 200 μm *outside the dip. In black we see the corrected coincidences inside the dip. I have corrected for the accidental coincidence following Eq.*(36)*. Clearly seen is the dip in the middle, as expected.*

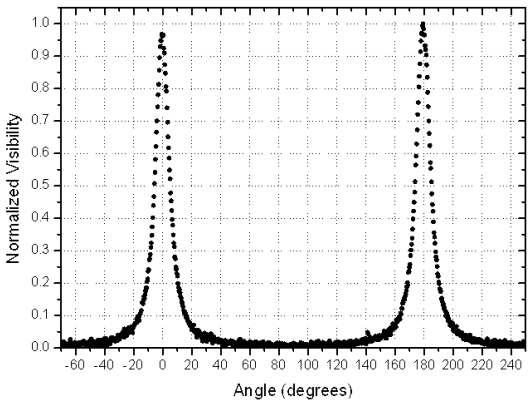

Figure 14: *The normalized visibility as a function of angle. We see a revival of the first peak at* 180^o*.*

called an accidental coincidence count. We correct this in the following way:

$$C^{Corrected} = Coincidence - Counts_{det1} \times Counts_{det2} \times 1,7ns \qquad (36)$$

We have compensated the effect of changes in interference due to misalignment by making a measurement of the coincides in the dip and a measurement of the coincides 200 μm outside the dip. We have used the coincides outside the dip as the maximum counts and the coincides inside the dip as minimum counts in order to get the Visibility:

$$Visibility = 1 - \frac{C_{dip}^{corrected}}{C_{outdip}^{corrected}} \tag{37}$$

This finally leads to what we call the "Normalized Visibility":

$$V_{normalized} = \frac{Visibility}{maximum(Visibility)} \tag{38}$$

Note that our normalized visibility always has a maximum value of 1 because we divide by the maximum of the visibility. The visibility we measure will not exceed 0.8, or 80%. This is due to combined spectral and spatial labeling of the entangled photons.

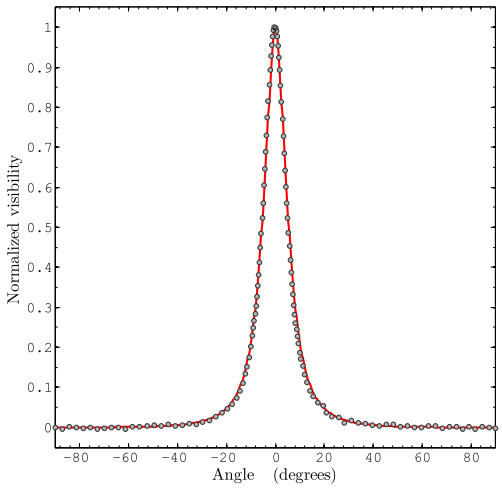

Figure 15: *The normalized visibility as a function of angle from the data of Fig. 13. We see a nice peak at the position of the dip. Shown are the measured points and the calculated theoretical red line. The measured points lay nicely on top of the theoretical curve, a beautiful result.*

From Fig.15 we can calculate the probability P_l of every OAM mode. As mentioned we can do this by making a Fourier transform of the measured

Visibility.

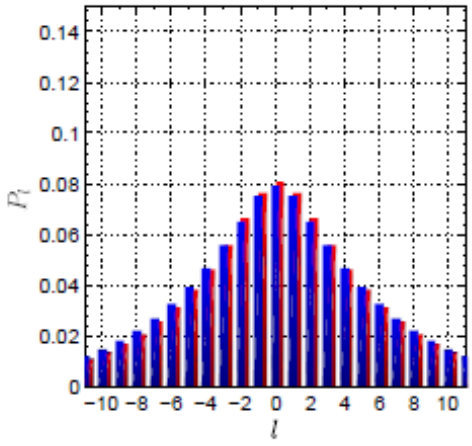

Figure 16: *The probability distribution as function of the orbital angular momentum number. Shown are the distribution calculated from the data of fig. 15 in blue and in red the theoretical distribution. Both almost coincide.*

We can calculate the number of orbital angular momentum modes of the generated photons, called the Smidt number: $K_{AZ} = \frac{1}{\sum_l P_l^2}$. Using our experimentally obtained data we calculated a Smidt number.

This is done by making a fourier transform of Fig. 15 to obtain Fig. 16, using Matlab. From this we calculated a Smidt number of 21.4 ± 0.5 If we compare this with the theoretical value, $K_{AZ} = 21.6$, we see that this is in good agreement within the experimental error.

5 Concluding discussion

We have demonstrated a powerful method for analyzing the orbital angular momentum of entangled photons by using a image rotator in a two-photon Mach-Zener interferometer (Hong-Ou-Mandel-type interference [15]). We have managed to obtain the required alignment precise; in the near field the beam displacement was less then 30 μm, in the far field the angular

displacement was 160 μrad. Further alignment was not possible because we had reached the mechanical limitations of our device. To improve this for future experiments, one should take a closer look to at mechanics of the rotator; but this was not necessary for the success of the experiment.

The experimental results were in good agreement with the theoretical predictions, as can be seen in Fig. 15 and Fig. 16. So we have succesfully deal with the challenge: "An experiment aimed at detecting the global OAM of the down-converted photon is a significant experimental challenge that is yet to be solved."

Looking back at the times in the lab, most of our efforts were in trying to figure out how the rotator works and how to align it properly. Eventually we have a procedure to align the rotator; we hope that this procedure will save some work in the future.

However some improvements can be made, like increasing the Visibility. As mentioned we could not exceed a visibility of 80% due to combined spectral and spatial labeling. If we would have used better filters in front of the photon counters, for instance a 1 nm bandpass filter centered at 826.2nm instead of a 2nm bandpass filter we would probably have measured ad higher visibility.

Furthermore we had some difficulties to find the expected constant Visibility V(θ) in the even-configuration. It looked as if the alignment was more crucial for this configuration. Where we thought mechanical deficiencies of the rotator were the problem for this setup, we had no problems with it in the odd-configuration. In the even-configuration we had to align manually for every small rotation of the rotator to stay at constant Visibility as function of angle.

In the odd geometry the visibility seemed to be much less sensitive to the alignment of the rotator and beam splitters; it could be measured relatively easily in the automatic setup. Why this is the case is something we didn't figure out but we know that it made our work much easier.

After I finished in the lab, more measurements where done by Henrique Di Lorenzo Pires. He investigated the visibility V(θ) and related OAM spectrum also for a 5 mm type II PPKTP crystal (this thesis uses a 2 mm type II crystal) and for a 5 mm thick type I crystal at different temperatures. These results will be submitted for publication.

References

[1] A. Goff,Am. J. Phys. **74**, 962 (2006)

[2] D.J. Griffiths, Introduction to Quantum Mechanics, 2nd edition, ISBN 0-13-191175-9

[3] G. Molina-Terriza, J.P. Torres and L. Torner, Nat. Phys. **3**, 305 (2007)

[4] C.C. Gerry and P.L.Knight, Introductory Quantum Optics, ISBN 0-521-52735-X

[5] A. Ekert and P.L. Knight, Am. J. Phys. **63**, 415 (1995)

[6] M.P. van Exter, P.S.K. Lee, S. Doesburg and J.P. Woerdman, Opt. Express **5**, 6431 (2007)

[7] D. Bru, Phys. Rev. Lett. **81**, 3018 (1998)

[8] H. H. Arnaut and G.A. Barbosa, Phys. Rev. Lett. **85**, 286 (2000)

[9] C.I. Osorio, Gabriel Molina-Terriza and Juan P. Torres, Phys. Rev. A **77**, 015810 (2008)

[10] S.P. Walborn, A.N. de Oliveira, R.S. Thebaldi and C.H. Monken, Phys. Rev. A **69**, 023811 (2004)

[11] J. Leach, B. Jack, J.Romero, M.Ritsch-Marte, R.W. Boyd, A.K. Jha, S.M. Barnett, S. Franke-Arnold and M.J. Padgett, Opt. Express **17**, 8287 (2009)

[12] M.P. van Exter, P.S.K. Lee, S. Doesburg, and J.P. Woerdman, Opt. Express **15**, 6431 (2007)

[13] W.H. Peeters, E.J.K. Verstegen and M.P. van Exter, Phys. Rev. A **76**, 042302 (2007)

[14] R.A.'Adams,C.Essex, Calculus-A complete course, 6th edition,ISBN 0-32-127000-2

[15] C.K. Hong,Z.Y. Ou and L. Mandel, Phys. Rev. Lett. **59**, 2044-2046 (1987)